

# K-dimensional trio coherent states

Hyo Seok Yi\*

Department of Physics, Korea Advanced Institute of Science and Technology,  
373-1 Guseong-dong, Yuseong-gu, Daejeon 305-701, Republic of Korea

Ba An Nguyen<sup>†</sup> and Jaewan Kim<sup>‡</sup>

School of Computational Sciences, Korea Institute for Advanced Study,  
207-43 Cheongryangni 2-dong, Dongdaemun-gu, Seoul 130-722, Republic of Korea

We introduce a novel class of higher-order, three-mode states called K-dimensional trio coherent states. We study their mathematical properties and prove that they form a complete set in a truncated Fock space. We also study their physical content by explicitly showing that they exhibit non-classical features such as oscillatory number distribution, sub-poissonian statistics, Cauchy-Schwarz inequality violation and phase-space quantum interferences. Finally, we propose an experimental scheme to realize the state with  $K = 2$  in the quantized vibronic motion of a trapped ion.

PACS numbers: 42.50.-p, 42.50.Vk, 32.80.Pj

## 1. Introduction

Higher-order effect as well as multimode nature of quantum states play a significant role in various physical applications. For instance, while multimode entangled states serve as necessary resources in multiuser quantum communication network (see, e.g., [1, 2, 3]), higher-order character gives rise to simultaneous squeezing in several directions [4, 5, 6] or to enhancement of antibunching [7], etc. Here we deal with states that are higher-order and three-mode.

The motivation for studying such states is twofold. Firstly, it is the academic motivation since we shall go on a route similar to those from 1-dimensional single-mode (two-mode) coherent states to  $K$ -dimensional single-mode [8, 9, 10, 11, 12, 13, 14] (two-mode [15, 16, 17, 18]) coherent states. Our study concerns the case of three modes thus generalizing the previously existing works. Our three-mode states are intrinsically nonclassical (see [19] for a comprehensive review). It is worth mentioning here that a number of nonclassical states are intimately linked with a symmetry group. But this does not compulsorily hold for all nonclassical states. For example, the  $N$ -mode sum-squeezed states [20, 21] are always (i.e., for any  $N \geq 2$ ) connected with the  $\text{su}(1,1)$  Lie algebra. Yet, the operators characterizing the  $N$ -mode difference-squeezed state [20, 22] forms a representation of the  $\text{su}(2)$  Lie algebra only for  $N = 2$ , not for  $N \geq 3$  [23]. The states we are going to study in this paper have no relation to a symmetry group. Secondly, the practical motivation could also be foreseen. As will be shown, a  $K$ -dimensional state is in fact a quantum superposition of  $K$  massive distinguishable substates. Such superpositions not only help to deeper understand the physics world both from quantum and classical point of view, but they may also serve as resources for quantum computation and quantum information processing. Moreover, our three-mode states are *naturally* entangled and, as such, they potentially promise wide applications. In this connection we notice that pair coherent states (PCS) [24], which are of two-mode entangled character, have been found useful in testing fundamental concepts of physics [25, 26, 27, 28] as well as in accomplishing quantum teleportation [29, 30]. We therefore do believe that there should be tasks (say, with participation of three parties like Fredkin or Toffoli gates and so on) which cannot be performed by single- or two-mode states but can be performed by three-mode ones such as ours.

The states of interest are defined as the eigenstates of the operator  $(\widehat{a}\widehat{b}\widehat{c})^K$ , with  $K$  a positive integer and  $\widehat{a}$  ( $\widehat{b}$ ,  $\widehat{c}$ ) the boson annihilation operator of mode  $a$  ( $b, c$ ), subject to the conditions that they be also the eigenstates of the operators  $\widehat{P} = \widehat{b}^\dagger\widehat{b} - \widehat{c}^\dagger\widehat{c}$  and  $\widehat{Q} = \widehat{a}^\dagger\widehat{a} - \widehat{c}^\dagger\widehat{c}$  corresponding to the differences of the number of quanta in the three modes. It is noted that the operators  $\widehat{a}$ ,  $\widehat{b}$  and  $\widehat{c}$  commute between each other. Denoting the state by  $|\xi, p, q\rangle_K$ , the three following equations must be simultaneously satisfied

$$(\widehat{a}\widehat{b}\widehat{c})^K |\xi, p, q\rangle_K = \xi^K |\xi, p, q\rangle_K, \quad (1)$$

$$\widehat{P} |\xi, p, q\rangle_K = p |\xi, p, q\rangle_K, \quad (2)$$

---

\*Electronic address: hsyi@muon.kaist.ac.kr

<sup>†</sup>Electronic address: nbaan@kias.re.kr; Corresponding author

<sup>‡</sup>Electronic address: jaewan@kias.re.kr

$$\widehat{Q} |\xi, p, q\rangle_K = q |\xi, p, q\rangle_K \quad (3)$$

where  $\xi = r \exp(i\varphi) \in \mathcal{C}$  and  $p, q$  are referred to as ‘‘charges’’ [31, 32] which, without loss of generality, are assumed to be non-negative. Equations (1) to (3) signify that a superposition of three-mode Fock states in the form

$$|\xi, p, q\rangle_K = \sum_{n=0}^{\infty} c_n |n+q\rangle_a |n+p\rangle_b |n\rangle_c \quad (4)$$

is a solution provided the coefficients  $c_n$  obey the constraint

$$c_{n+K} = \sqrt{\frac{(n+q)!(n+p)!n!}{(n+q+K)!(n+p+K)!(n+K)!}} \xi^K c_n. \quad (5)$$

This constraint forms  $K$  independent strings  $\{s_0, s_1, \dots, s_{K-1}\}$  where each of  $s_j$  consists of an infinite number of related coefficients  $s_j = \{c_j, c_{j+K}, c_{j+2K}, \dots\}$  with  $c_j$  being the representative of the  $s_j$ -string. The states  $|\xi, p, q\rangle_K$  are therefore highly degenerate since the representatives  $c_0, c_1, \dots, c_{K-1}$  remain arbitrary. We now impose conditions on the representative  $c_j$  so that a state  $|\xi, p, q\rangle_{Kj}$  associated with the coefficients taken from the  $s_j$ -string be normalized to unity. (Note that the subscript  $Kj$  should not be conceived as a single index; it refers to two separate integers  $K$  and  $j$ .) Then, each state  $|\xi, p, q\rangle_{Kj}$  with a fixed  $j \in [0, K-1]$  has the following explicit Fock expansion

$$|\xi, p, q\rangle_{Kj} = N_{Kj}(r^2, p, q) \sum_{n=0}^{\infty} \frac{\xi^{Kn+j}}{\sqrt{\rho_{pq0}(Kn+j)}} |Kn+j+q\rangle_a |Kn+j+p\rangle_b |Kn+j\rangle_c \quad (6)$$

where

$$\rho_{pq0}(Kn+j) = (Kn+j+p)!(Kn+j+q)!(Kn+j)! \quad (7)$$

and

$$N_{Kj}(x, p, q) = \left( \sum_{m=0}^{\infty} \frac{x^{Km+j}}{\rho_{pq0}(Km+j)} \right)^{-1/2} \quad (8)$$

is the normalization coefficient. Since the overlap between states  $|\xi, p, q\rangle_{Kj}$  and  $|\xi', p', q'\rangle_{Kj'}$  is determined by

$${}_{Kj'} \langle \xi', p', q' | \xi, p, q \rangle_{Kj} = \delta_{jj'} \delta_{pp'} \delta_{qq'} \frac{N_{Kj}(\xi'^*, p, q) N_{Kj}(\xi, p, q)}{N_{Kj}^2(\sqrt{\xi'^* \xi}, p, q)} \quad (9)$$

it follows that the normalized states  $|\xi, p, q\rangle_{Kj}$  are orthogonal with respect to  $j, p, q$  but non-orthogonal with respect to  $\xi$ . It is worth emphasizing that for a given  $K$  there are  $K$  states  $|\xi, p, q\rangle_{Kj}$  ( $j = 0, 1, \dots, K-1$ ) each of which is a three-mode entangled state. In other words, the eigenvalue set  $\{\xi^K, p, q\}$  is  $K$ -degenerate corresponding to  $K$  linearly independent eigenstates  $|\xi, p, q\rangle_{Kj}$ . We call them  $K$ -dimensional trio coherent states (KTCS's) because the dimension of the space spanned by these states is  $K$  even though each of them is embedded in a vector space of infinite dimension characterized by the complex variable  $\xi$ . In the same spirit, multidimensional entangled coherent states have also been investigated recently in [33] where they prove to be necessary for teleportation of quantum states of a particular kind. When  $K = 1$  the KTCS reduces to the trio coherent state (TCS) introduced in [34] which is a generalization of the PCS [24]. So, in what follows, when KTCS's are quoted it implies  $K > 1$ .

In the next part of this paper we first expose mathematical properties of the KTCS including proof of their (over)completeness. Physical properties are then studied showing that KTCS's are inherently nonclassical. Finally, we propose an experimental scheme to produce a KTCS in the vibrational motion of the center-of-mass of an ion trapped in real space by a three-dimensional harmonic potential.

## 2. Mathematical properties

States  $|\xi, p, q\rangle_{Kj}$  with different  $j$  can be transformed from one to another by a “rotation” operator  $\widehat{R}_{Klm}(\xi, p, q)$  defined by

$$\widehat{R}_{Klm}(\xi, p, q) = \frac{N_{Kl}(r^2, p, q)}{N_{Km}(r^2, p, q)} \xi^{-[m-l]_K} (\widehat{a}\widehat{b}\widehat{c})^{[m-l]_K} \quad (10)$$

where  $[x]_K = x$  if  $x \geq 0$  and  $[x]_K = x + K$  if  $x < 0$ . That is, for any  $l, m \in [0, K-1]$ ,

$$|\xi, p, q\rangle_{Kl} = \widehat{R}_{Klm}(\xi, p, q) |\xi, p, q\rangle_{Km}. \quad (11)$$

Another important property is: any KTCS can be expressed as a superposition of  $K$  phase-correlated TCS's. Namely,

$$|\xi, p, q\rangle_{Kj} = \frac{N_{Kj}(r^2, p, q)}{KN(r^2, p, q)} \sum_{j'=0}^{K-1} \exp\left(-\frac{2\pi i}{K} jj'\right) |\xi_{Kj'}, p, q\rangle \quad (12)$$

where  $|\xi, p, q\rangle \equiv |\xi, p, q\rangle_{10}$ ,  $N(r^2, p, q) \equiv N_{10}(r^2, p, q)$  and

$$\xi_{Kj} = \xi \exp\left(\frac{2\pi ij}{K}\right). \quad (13)$$

The expansion (12) can be straightforwardly verified by virtue of the identities  $\sum_{m=0}^{K-1} \exp[2\pi i(l-l')m/K] \equiv K\delta_{ll'}$  and  $\sum_{m=0}^{\infty} X_m |m\rangle \equiv \sum_{l=0}^{K-1} \sum_{n=0}^{\infty} X_{nK+l} |nK+l\rangle$ . It can be noted, due to Eq. (13), that the TCS's superposing a KTCS are evenly distributed on a circle of radius  $r$  in the phase space. The inverse transformation of (12) is

$$|\xi_{Kj}, p, q\rangle = N(r^2, p, q) \sum_{j'=0}^{K-1} \frac{\exp\left(\frac{2\pi i}{K} jj'\right)}{N_{Kj'}(r^2, p, q)} |\xi, p, q\rangle_{Kj'}. \quad (14)$$

Alternatively, making a change  $\{\xi_{Kj} \equiv \xi \exp(2\pi ij/K) \rightarrow \chi, \xi \rightarrow \chi \exp(-2\pi ij/K)\}$  in (14) and taking into account the identity

$$|\chi \exp(-2\pi ij/K), p, q\rangle_{Kj'} \equiv \exp(-2\pi ij'/K) |\chi, p, q\rangle_{Kj'} \quad (15)$$

which can be easily checked by use of the Fock representation (6) in both sides of (15), we can cast (14) into a simpler but more convenient form (after changing  $\chi$  back to  $\xi$ ) as

$$|\xi, p, q\rangle = N(r^2, p, q) \sum_{j=0}^{K-1} \frac{|\xi, p, q\rangle_{Kj}}{N_{Kj}(r^2, p, q)}. \quad (16)$$

More interestingly, it turns out that KTCS's of any two different dimensions are also related to each other. A hint to establish such a relation is first using (12) to express a KTCS with a given  $K$  in terms of TCS's and then applying (16) to get the TCS's back in terms of K'TCS's with a different  $K'$  (generally  $K' \neq K$ ). As a result, we arrive at

$$|\xi, p, q\rangle_{Kj} = \frac{N_{Kj}(x, p, q)}{K} \sum_{j'=0}^{K'-1} \sum_{j''=0}^{K-1} \frac{\exp\left(-\frac{2\pi i}{K} jj''\right)}{N_{K'j'}(x, p, q)} |\xi_{Kj' j''}, p, q\rangle_{K'j'}. \quad (17)$$

The transformation (17) is most general in the sense that it recovers (12) when  $K' = 1, j' = 0$  and (16) when  $K = 1, j = 0$ . In the special case, when  $K' = K$ , the r.h.s. of (17) becomes nothing else but its l.h.s., as it should be.

In terms of the usual single-mode coherent state

$$|\eta\rangle \equiv \exp(-|\eta|^2/2) \sum_{n=0}^{\infty} \frac{\eta^n}{\sqrt{n!}} |n\rangle, \quad (18)$$

the following expansion holds in general

$$|\xi, p, q\rangle_{Kj} = N_{Kj}(r^2, p, q) \int \frac{\alpha^{*q} d^2\alpha}{\pi} \int \frac{\beta^{*p} d^2\beta}{\pi} \int \frac{d^2\gamma}{\pi} N_{Kj}^{-2}(\xi\alpha^*\beta^*\gamma^*, p, q) \\ \times \exp[-(|\alpha|^2 + |\beta|^2 + |\gamma|^2)/2] |\alpha\rangle_a |\beta\rangle_b |\gamma\rangle_c \quad (19)$$

because of the completeness of the coherent state. In particular, however, a formula via three phase-correlated coherent states whose amplitudes  $\alpha$ ,  $\beta$  and  $\gamma$  satisfy the equality  $\alpha\beta\gamma = \xi$  seems to be more useful. That looks like this

$$|\xi, p, q\rangle_{Kj} = \frac{1}{K} N_{Kj}(r^2, p, q) \exp[(|\alpha|^2 + |\beta|^2 + |\gamma|^2)/2] \\ \times \sum_{j'=0}^{K-1} \frac{\exp(-\frac{2\pi i}{K} jj')}{\alpha_{Kj'}^q \beta_{Kj'}^p} \int_0^{2\pi} \frac{d\theta}{2\pi} \int_0^{2\pi} \frac{d\theta'}{2\pi} \exp[-i(q\theta + p\theta')] \\ \times |\alpha_{Kj'} \exp(i\theta)\rangle_a |\beta_{Kj'} \exp(i\theta')\rangle_b |\gamma_{Kj'} \exp[-i(\theta + \theta')]\rangle_c. \quad (20)$$

In fact, when  $K = 1$ ,  $j = 0$  and  $\alpha = \beta = \gamma = \xi^{1/3}$ , formula (20) reduces to formula (1) in [35].

We now turn to the important issue of proving that the  $K$  states  $|\xi, p, q\rangle_{Kj}$  ( $j = 0, 1, \dots, K-1$ ) form a complete set. As seen from (6), any state  $|\xi, p, q\rangle_{Kj}$  spans the three-mode Fock space in which the  $q$  ( $p$ ) first number states of mode  $a$  ( $b$ ) with  $n_a = 0, 1, \dots, q-1$  ( $n_b = 0, 1, \dots, p-1$ ) are lacking. In such a truncated Fock space the unity operator has to be of the form (similar matter associated with single-mode photon-added coherent states can be found in [36])

$$\mathbf{I}_{p,q} = \sum_{n=0}^{\infty} |n+q\rangle_a |n+p\rangle_b |n\rangle_c \langle n|_b \langle n+p|_a \langle n+q|. \quad (21)$$

The resolution of unity of the KTCS's then amounts to existence of a weight function  $W_{Kj}(|\xi|^2, p, q)$  such as to fulfill the following completeness condition

$$\sum_{j=0}^{K-1} \int d^2\xi |\xi, p, q\rangle_{Kj} W_{Kj}(|\xi|^2, p, q)_{Kj} \langle \xi, p, q| = \mathbf{I}_{p,q}. \quad (22)$$

To solve for  $W_{Kj}(|\xi|^2, p, q)$  we substitute  $\xi = r \exp(i\varphi)$  and (6) into (22) and integrate over  $\varphi$ . After the  $\varphi$ -integration the function  $W_{Kj}(r^2, p, q)$  is looked for in the form

$$W_{Kj}(r^2, p, q) = \frac{\widetilde{W}(r^2, p, q, 0)}{\pi N_{Kj}^2(r^2, p, q)}, \quad (23)$$

where  $\widetilde{W}(r^2, p, q, 0)$  is to be determined from the equation

$$\int_0^{\infty} \widetilde{W}(x, p, q, 0) x^n dx = \rho_{pq0}(n); \quad n = 0, 1, 2, \dots, \infty. \quad (24)$$

This is the classical Stieltjes power-moment problem [37], with the set of  $n$ -th moments  $\rho_{pq0}(n)$  parameterized by  $\{p, q, 0\}$ . If  $n$  in Eq. (24) is extended to  $s-1$  where  $s \in \mathcal{C}$ , then our problem can be formulated in terms of the Mellin and inverse Mellin transforms [38, 39] which have been extensively used in the context of various kinds of generalized coherent states [40, 41, 42, 43, 44, 45]. Here,  $\rho_{pq0}(s-1)$  is the Mellin transform,  $\mathcal{M}[\widetilde{W}(x, p, q, 0); s]$ , of  $\widetilde{W}(x, p, q, 0)$ , i.e.

$$\rho_{pq0}(s-1) = \mathcal{M}[\widetilde{W}(x, p, q, 0); s] := \int_0^{\infty} \widetilde{W}(x, p, q, 0) x^{s-1} dx \quad (25)$$

and,  $\widetilde{W}(x, p, q, 0)$  in turn is the inverse Mellin transform,  $\mathcal{M}^{-1}[\rho_{pq0}(s-1); x]$ , of  $\rho_{pq0}(s-1)$ , i.e.

$$\widetilde{W}(x, p, q, 0) = \mathcal{M}^{-1}[\rho_{pq0}(s-1); x] := \frac{1}{2\pi i} \int_{-i\infty}^{i\infty} \rho_{pq0}(s-1) x^{-s} ds. \quad (26)$$

We know [44] that the solution of the simpler problem

$$\int_0^\infty \widetilde{W}(x, l) x^n dx = \rho_l(n) = (n + l)!, \quad (27)$$

is given by

$$\widetilde{W}(x, l) = \mathcal{M}^{-1}[\rho_l(s - 1); x] = x^l e^{-x}. \quad (28)$$

To make use of the known result (28) we twice apply the Parseval relation [38, 39] which we reformulate for our purpose here in the form

$$\mathcal{M}^{-1}[f(s - 1)g(s - 1); x] = \int_0^\infty \frac{dt}{t} \mathcal{M}^{-1}[f(s - 1); t] \mathcal{M}^{-1}[g(s - 1); \frac{x}{t}]. \quad (29)$$

Now, by virtue of (26), (27) and (29), we have immediately

$$\begin{aligned} \widetilde{W}(x, p, q, 0) &= \mathcal{M}^{-1}[\rho_{pq0}(s - 1); x] \equiv \mathcal{M}^{-1}[\rho_p(s - 1)\rho_q(s - 1)\rho_0(s - 1); x] \\ &= \int_0^\infty \frac{dt}{t} \mathcal{M}^{-1}[\rho_p(s - 1)\rho_q(s - 1); t] \mathcal{M}^{-1}[\rho_0(s - 1); \frac{x}{t}] \\ &= \int_0^\infty \frac{dt}{t} \left[ \int_0^\infty \frac{d\tau}{\tau} \mathcal{M}^{-1}[\rho_p(s - 1); \tau] \mathcal{M}^{-1}[\rho_q(s - 1); \frac{t}{\tau}] \right] \mathcal{M}^{-1}[\rho_0(s - 1); \frac{x}{t}] \\ &= \int_0^\infty t^{q-1} e^{-x/t} \left[ \int_0^\infty \tau^{p-q-1} e^{-\tau-t/\tau} d\tau \right] dt \end{aligned} \quad (30)$$

where in the last step we made use of Eq. (28). Performing the  $\tau$ -integration we finally arrive at

$$\widetilde{W}(x; p, q, 0) = \int_0^\infty t^{-1+(p+q)/2} e^{-x/t} K_{q-p}(2\sqrt{t}) dt \quad (31)$$

where  $K_n(t) = K_{-n}(t) = K_{|n|}(t)$  stands for the modified Bessel function of the second kind. There are two remarks to be made at this point as follows.

- The condition (22) is that of over-completeness rather than completeness. This is due to the non-orthogonality of KTCS's with respect to  $\xi$  and is explicitly reflected by the fact that any state  $|\xi, p, q\rangle_{Kj}$  can be represented via the others as

$$|\xi, p, q\rangle_{Kj} = N_{Kj}(\xi, p, q) \int d^2\xi' \frac{N_{Kj}(\xi'^*, p, q) W_{Kj}(|\xi'|^2, p, q)}{N_{Kj}^2(\sqrt{\xi'^* \xi}, p, q)} |\xi', p, q\rangle_{Kj}. \quad (32)$$

- The solution (31) is not unique. According to the Carleman's (sufficient) condition [46], our solution would be unique (non-unique) if the sum  $S = \sum_{n=1}^\infty S_n$ , with  $S_n = [(Kn + j + q)!(Kn + j + p)!(Kn + j)!]^{-1/2n}$ , diverges (converges). We now apply the logarithmic test [47] to examine the convergence of  $S$ . The logarithmic criterion says that if  $T = \lim_{n \rightarrow \infty} \ln(S_n)/\ln(n) > -1$  ( $< -1$ ) then  $S$  diverges (converges). To calculate  $T$  we rewrite  $S_n$  in terms of Gamma functions,  $S_n = [\Gamma(Kn + j + q + 1)\Gamma(Kn + j + p + 1)\Gamma(Kn + j + 1)]^{-1/2n}$ , and then use the Stirling's formula,  $\Gamma(Kn + l) \approx \sqrt{2\pi} \exp(-Kn)(Kn)^{Kn}$ , which is valid for large  $n$  and finite  $l$  ( $l \ll n$ ). As a result, we obtain  $\lim_{n \rightarrow \infty} \ln(S_n) = -3K \ln(n)/2$  and, hence,  $T = -3K/2 < -1$  for any positive integers  $K$ . This proves the non-uniqueness of our solution (31).

To end this section we remind from (6) that the KTCS's are normalized by the normalization coefficient  $N_{Kj}(r^2, p, q)$  determined by (8). The states are also continuous in the variable  $\xi$  because  $\left| |\xi, p, q\rangle_{Kj} - |\xi', p, q\rangle_{Kj} \right|^2 = 2 \left[ 1 - \text{Re} \left( \langle \xi', p, q | \xi, p, q \rangle_{Kj} \right) \right]$  tends to vanish when  $|\xi - \xi'| \rightarrow 0$ , as is evident from (8) and (9). Furthermore, as followed from (23) and (31), the weight function  $W_{Kj}(|\xi|^2, p, q)$  in (22) is guaranteed to be positive (thanks to positivity of the Bessel function  $K_n(t)$ ). Therefore, the minimal set of conditions [48, 49] required for an ensemble of

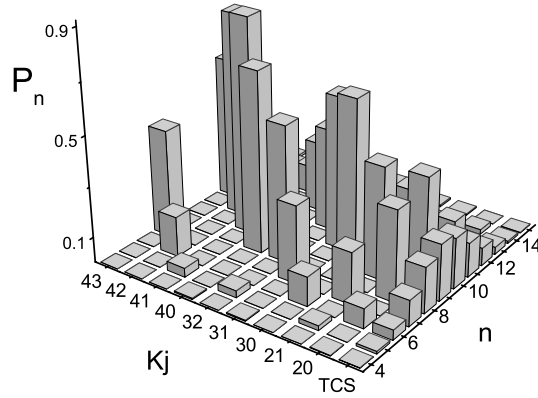


FIG. 1: 3D bar plot showing oscillation of the number distribution,  $P_n(\xi, p, q, K, j)$ , for  $r = 30, p = q = 0$  and different combinations of  $Kj$ . For comparison, also plotted is the case of TCS which does not oscillate at all.

states to be *coherent* is met for the KTCS's. That explains why “*coherent*” arises in naming the states  $|\xi, p, q\rangle_{Kj}$  as “*K-dimensional trio coherent states*” of which “*coherent*” must be family name and “*K-dimensional trio*” first name.

### 3. Physical content

In this section we explore the physical content of the KTCS's. The probability of finding  $l$  ( $m, n$ ) quanta of mode  $a$  ( $b, c$ ) in state  $|\xi, p, q\rangle_{Kj}$  is given by

$$P_{lmn}(\xi, p, q, K, j) = |{}_{Kj}\langle \xi, p, q | l, m, n \rangle_{abc}|^2 = P_n(\xi, p, q, K, j) \delta_{m, n+p} \delta_{l, n+q} \quad (33)$$

with

$$P_n(\xi, p, q, K, j) = \frac{r^{2n} N_{Kj}^2(r^2, p, q) I(\frac{n-j}{K})}{\rho_{pq0}(n)} \quad (34)$$

where  $I(x) = 1$  if  $x$  is an integer and  $I(x) = 0$  if  $x$  is a non-integer. While the Kronecker symbols in (33) reveal the entanglement of the modes in state  $|\xi, p, q\rangle_{Kj}$ , the function  $I(\frac{n-j}{K})$  in (34) indicates that for any  $K > 1$  the number distribution of state  $|\xi, p, q\rangle_{Kj}$  suffers an oscillation as shown in Fig. 1 in which the TCS is also plotted that does not oscillate at all.

Further information on inherent quantum statistics of state  $|\xi, p, q\rangle_{Kj}$  can be obtained from the Mandel parameter  $M_x$  for mode  $x$  [50]

$$M_x = \frac{\langle \hat{n}_x^{(2)} \rangle - \langle \hat{n}_x \rangle^2}{\langle \hat{n}_x \rangle} \quad (35)$$

where  $\hat{n}_x = \hat{x}^\dagger \hat{x}$  with  $\hat{x}$  the annihilation operator of mode  $x$  and the expectation value of the factorial moment of the number operator  $\langle \hat{n}_x^{(l)} \rangle \equiv \langle \prod_{m=0}^{l-1} (\hat{n}_x - m) \rangle$  is derived for our KTCS's in the form

$$\langle \hat{n}_a^{(l)} \rangle = z^{l-q} N_{Kj}^2 \frac{d^l}{dz^l} \left( \frac{z^q}{N_{Kj}^2} \right), \quad (36)$$

$$\langle \hat{n}_b^{(l)} \rangle = z^{l-p} N_{Kj}^2 \frac{d^l}{dz^l} \left( \frac{z^p}{N_{Kj}^2} \right), \quad (37)$$

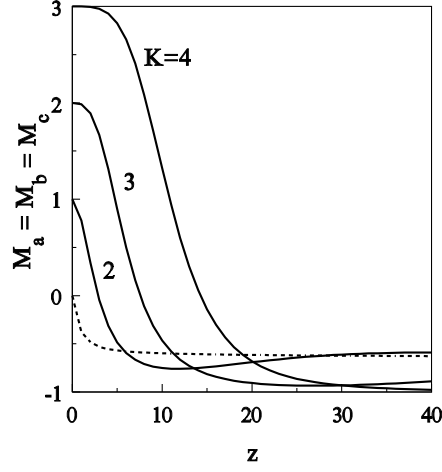


FIG. 2: Mandel parameters  $M_a = M_b = M_c$  versus  $z = r^2$  for  $j = p = q = 0$  and different  $K$  indicated near the curve. For comparison, also plotted is the case of TCS (dashed curve) which remains sub-poissonian in the whole range of  $z$ .

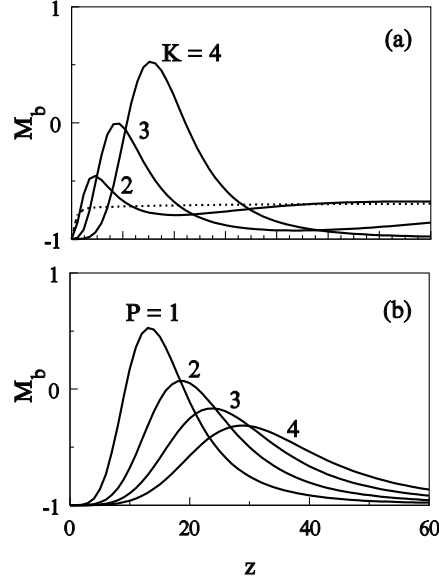


FIG. 3: Mandel parameter  $M_b$  versus  $z$  for  $j = q = 0$  while (a)  $p = 1$  and  $K = 2, 3, 4$ ; (b)  $K = 4$  and  $p = 1, 2, 3, 4$ . The dashed curve in (a) is the case of TCS which exhibits no maxima.

$$\langle \hat{n}_c^{(l)} \rangle = z^l N_{Kj}^2 \frac{d^l}{dz^l} \left( \frac{1}{N_{Kj}^2} \right), \quad (38)$$

where  $N_{Kj} \equiv N_{Kj}(z, p, q)$  and  $z = r^2$ . An evident factor that makes difference between modes is the charges  $p, q$ . For  $p = q = 0$  all the three modes are “identical”. For  $p > q = 0$  ( $q > p = 0$ ) mode  $a$  ( $b$ ) and mode  $c$  behave identically which are however distinct from mode  $b$  ( $a$ ). For  $p = q > 0$  modes  $a$  and  $b$  are similar while mode  $c$  is dissimilar. Only when  $p \neq q$  and each of them acquires a positive integer the three modes are well distinguishable one from another.

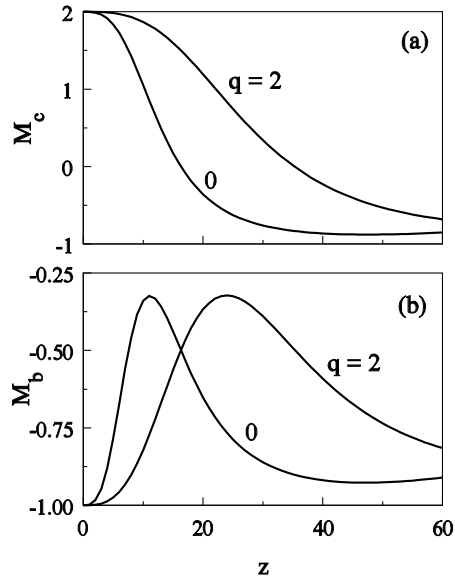


FIG. 4: Mandel parameters (a)  $M_c$  and (b)  $M_b$  versus  $z$  for  $K = 3$ ,  $j = 0$ ,  $p = 2$  while  $q = 0$  and  $q = 2$ .

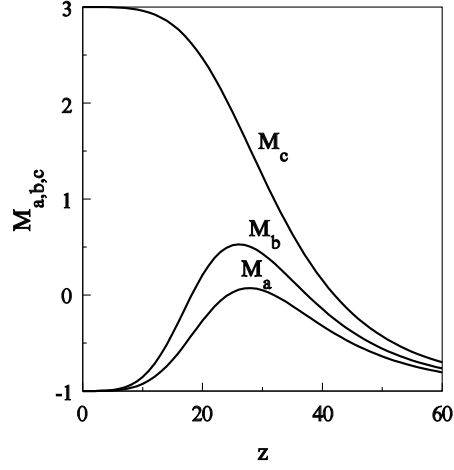


FIG. 5: Mandel parameters  $M_a$ ,  $M_b$  and  $M_c$  versus  $z$  for  $K = 4$ ,  $j = 0$ ,  $p = 1$  and  $q = 2$ .

Use of (36) in (35) yields explicitly

$$M_a = \frac{2z^2 (N_{Kj} N''_{Kj} - N'^2_{Kj}) + q N^2_{Kj}}{2z N_{Kj} N'_{Kj} - q N^2_{Kj}}, \quad (39)$$

$$M_b = \frac{2z^2 (N_{Kj} N''_{Kj} - N'^2_{Kj}) + p N^2_{Kj}}{2z N_{Kj} N'_{Kj} - p N^2_{Kj}}, \quad (40)$$



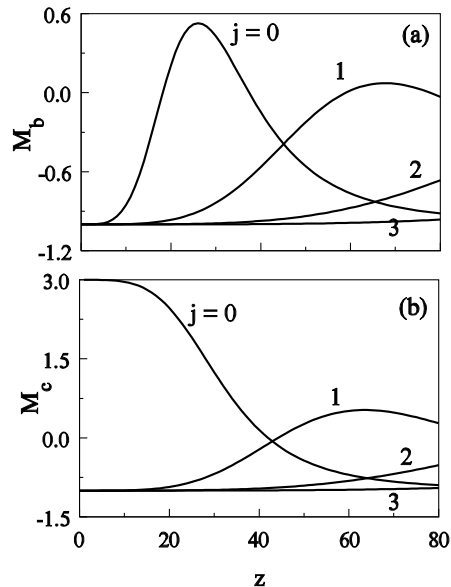


FIG. 6: Mandel parameters (a)  $M_b$  and (b)  $M_c$  versus  $z$  for  $K = 4$ ,  $j = 0, 1, 2, 3$ ,  $p = 1$  and  $q = 2$ .

$$M_c = \frac{z \left( N_{Kj} N''_{Kj} - N'^2_{Kj} \right)}{N_{Kj} N'_{Kj}} \quad (41)$$

where  $N'_{Kj} \equiv dN_{Kj}/dz$  and  $N''_{Kj} \equiv d^2 N_{Kj}/dz^2$ .

In Fig. 2 we plot  $M_c$  as a function of  $z$  for  $j = p = q = 0$  and different  $K$ . Contrary to the TCS for which mode  $c$  remains sub-poissonian (i.e.  $M_c < 0$ ) in the whole range of  $z$ , for KTCS's the mode is super-poissonian (i.e.  $M_c > 0$ ) at small values of  $z$  but then becomes sub-poissonian when  $z$  increases. The crossover point  $z_{cross}$  at which the statistics changes from super- to sub-poissonian moves to the right for greater values of  $K$ . At large values of  $z$  the mode gets more antibunched in a higher dimension.

For  $p > q = 0$  the shape of  $M_c = M_a$  looks like that in Fig. 2 but for a fixed  $K$  the crossover point  $z_{cross}$  shifts to the large- $z$  side with increasing  $p$ . For instance, when  $K = 3$  numerical calculations give  $z_{cross} = 7.5628, 12.0114, 16.3108$  and  $20.5606$  for  $p = 0, 1, 2$  and  $3$ , respectively. Concerning mode  $b$ , its behavior is qualitatively different as displayed in Fig. 3. Contrary to the TCS for which  $M_b$  monotonically increases with  $z$ , for KTCS's it exhibits a maximum which may be located in the super-poissonian domain if the dimension  $K$  is high enough (e.g., if  $K \geq 4$  when  $p = 1$  as illustrated in Fig. 3 (a)). The effect of the charge  $p$  is to pull down and right-shift the whole curve (see Fig. 3 (b)) so that for a given  $K$  the mode can be made entirely sub-poissonian (if it was not so) by setting  $p$  large enough (see, e.g., Fig. 3 (b) for  $K = 4$ :  $M_b < 0$  in the whole range of  $z$  when  $p \geq 3$ ).

For  $p = q > 0$ , as mentioned above,  $M_a = M_b \neq M_c$ . Compared to the situation  $p > q = 0$  the following properties hold. For mode  $c$  we find the relation  $M_c(K, p = q > 0) > M_c(K, p > q = 0)$  in the whole range of  $z$  except for  $z = 0$  at which  $M_c(K, p = q > 0) = M_c(K, p > q = 0)$ , as seen from Fig. 4 (a). For mode  $b$  (a) we find that  $\max[M_b(K, p = q > 0)] = \max[M_b(K, p > q = 0)]$  but the maximum of  $M_b(K, p > q = 0)$  appears "earlier" than that of  $M_b(K, p = q > 0)$  when  $z$  is increasing (see Fig. 4 (b)).

For  $p > 0, q > 0$  and  $p \neq q$  each mode develops its own dependence on the parameters and are well distinguishable as Fig. 5 shows.

The specific feature of KTCS's is their degeneracy as explained in Section 1. A given manifold characterized by a fixed  $K > 1$  consists of  $K$  eigenstates enumerated by the parameter  $j = 0, 1, 2, \dots, K - 1$ . States with the same  $K$  but different  $j$  differ in their number distribution which is dictated by the Kronecker symbols in Eq. (33) and by the function  $I\left(\frac{n-j}{K}\right)$  in Eq. (34). These mean that one cannot find  $n$  quanta of mode  $c$  ( $b, a$ ) in state  $|\xi, p, q\rangle_{Kj}$  if  $n - j$  ( $n - j - p, n - j - q$ ) is not a multiple of  $K$  (see Fig. 1, for verification). States with the same  $K$  but different  $j$  differ also in their quantum statistics. So far (in Figs. 2 to 5) we have treated only  $j = 0$  in which case, for arbitrary  $K, p$  and  $q$ , we have  $M_c(j = 0, z \rightarrow 0) \rightarrow K - 1$  and  $M_{a,b}(j = 0, z \rightarrow 0) \rightarrow -1$ . For  $j > 0$ , however, all the three modes are highly antibunched at small values of  $z$  independent of  $K, p$  and  $q$ , i.e.  $M_{a,b,c}(j > 0, z \rightarrow 0) \rightarrow -1$ . Also,

at small  $z$  a state with greater  $j$  has higher degree of antibunching, i.e. its number distribution profile is narrower. Those observations are demonstrated in Fig. 6.

Another intriguing figure of merit is strong correlations between modes of KTCS's. Such correlations are expected to be nonclassical. To verify it we examine the Cauchy-Schwarz inequality (CSI) [51] which describes a classical correlation between two modes  $x$  and  $y$

$$J_{xy} = \langle \hat{n}_x^{(2)} \rangle \langle \hat{n}_y^{(2)} \rangle - \langle \hat{n}_x \hat{n}_y \rangle^2 \geq 0. \quad (42)$$

General expressions for expectation values of products of two factorial moments  $\hat{n}_x^{(l)} \hat{n}_y^{(m)}$  can also be analytically derived for our KTCS's in terms of the normalization coefficient (8). As a result of derivation, we arrive at

$$\langle \hat{n}_a^{(l)} \hat{n}_b^{(m)} \rangle = z^{m-p} N_{Kj}^2 \frac{d^m}{dz^m} \left[ z^{l+p-q} \frac{d^l}{dz^l} \left( \frac{z^q}{N_{Kj}^2} \right) \right], \quad (43)$$

$$\langle \hat{n}_a^{(l)} \hat{n}_c^{(m)} \rangle = z^m N_{Kj}^2 \frac{d^m}{dz^m} \left[ z^{l-q} \frac{d^l}{dz^l} \left( \frac{z^q}{N_{Kj}^2} \right) \right], \quad (44)$$

$$\langle \hat{n}_b^{(l)} \hat{n}_c^{(m)} \rangle = z^{l-p} N_{Kj}^2 \frac{d^l}{dz^l} \left[ z^{m+p} \frac{d^m}{dz^m} \left( \frac{1}{N_{Kj}^2} \right) \right]. \quad (45)$$

Use of (36) and (43) - (45) in (42) yields explicitly

$$\begin{aligned} J_{ab} = & N_{Kj}^{-3} \{ pq(1-p-q)N_{Kj}^3 + 24z^3 N_{Kj}^{\prime 3} \\ & - 2z^2 N_{Kj} N_{Kj}' [(2+7(p+q)-(p-q)^2)N_{Kj}' + 4zN_{Kj}''] \\ & + 2zN_{Kj}^2 [6pqN_{Kj}' + z(p+q-(p-q)^2)N_{Kj}'] \}, \end{aligned} \quad (46)$$

$$J_{ac} = 2z^2 N_{Kj}^{-3} \{ 12zN_{Kj}^{\prime 3} + q(1-q)N_{Kj}^2 N_{Kj}'' - N_{Kj} N_{Kj}' [(2+7q-q^2)N_{Kj}' + 4zN_{Kj}'] \}, \quad (47)$$

$$J_{bc} = 2z^2 N_{Kj}^{-3} \{ 12zN_{Kj}^{\prime 3} + p(1-p)N_{Kj}^2 N_{Kj}'' - N_{Kj} N_{Kj}' [(2+7p-p^2)N_{Kj}' + 4zN_{Kj}'] \}. \quad (48)$$

It is well-known that a nonclassical correlation violates the CSI [52], i.e. it makes  $J_{xy} < 0$ . To assess degree of CSI violation we scale  $J_{xy}$  to  $\langle \hat{n}_x \hat{n}_y \rangle^2$ , i.e. we use a quantity  $G_{xy}$  defined by

$$G_{xy} = \frac{J_{xy}}{\langle \hat{n}_x \hat{n}_y \rangle^2} \quad (49)$$

as a measure of CSI violation. For states with  $j > 0$  (i.e.  $j = 1, 2, \dots, K-1$ ) we find that the CSI is always violated. However, for  $j = 0$ , though the TCS also always violates the CSI, the KTCS's do not. The violation depends on the type of correlation and the value of charges  $p, q$ . The simulation reveals that  $G_{ab}$  is always negative but  $G_{ac}$  and  $G_{bc}$  may be positive depending on the charges. More concretely, when both  $p$  and  $q$  are not greater than one we find that  $G_{xy} < 0 \forall x, y, K, z$ , i.e. the CSI is fully violated. However, when  $p$  ( $q$ ) = 1 and  $q$  ( $p$ )  $\geq 2$  the quantity  $G_{bc}$  ( $G_{ac}$ ) remains always negative but  $G_{ac}$  ( $G_{bc}$ ) becomes positive at small values of  $z$  and the higher the dimension  $K$  the wider the  $z$ -domain within which the CSI is not violated, i.e. there is a partial violation of the CSI. Those behaviors are illustrated in Fig. 7. Finally, when both  $p \geq 2$  and  $q \geq 2$ , both the quantities  $G_{bc}$  and  $G_{ac}$  violate the CSI only partially in the sense mentioned above.

We next study the phase-space characteristics of the KTCS's. For that purpose we consider the three-mode Q-function defined as [53]

$$Q_{\xi pq}^{Kj}(\alpha, \beta, \gamma) = \frac{1}{\pi^3} \left| {}_{abc}(\alpha, \beta, \gamma | \xi, p, q)_{Kj} \right|^2 \quad (50)$$

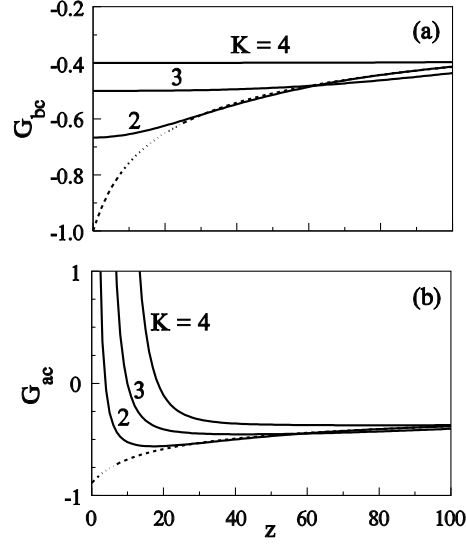


FIG. 7: Correlation measures (a)  $G_{bc}$  and (b)  $G_{ac}$  versus  $z$  for  $j = 0, p = 1, q = 2$  and different  $K$  as indicated near the curve. For comparison, also plotted is the case of TCS (dashed curve) which remains negative in the whole range of  $z$ .

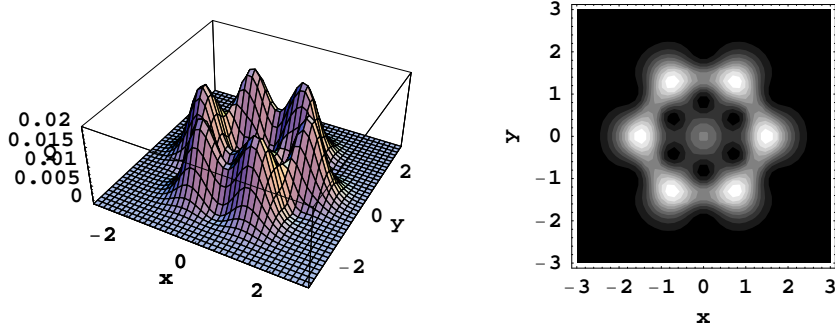


FIG. 8: Function  $Q = \pi^3 Q_{\xi pq}^{Kj}(x, y)$  and its contour plot for  $\xi = 5, p = q = 0, K = 2$  and  $j = 0$ .

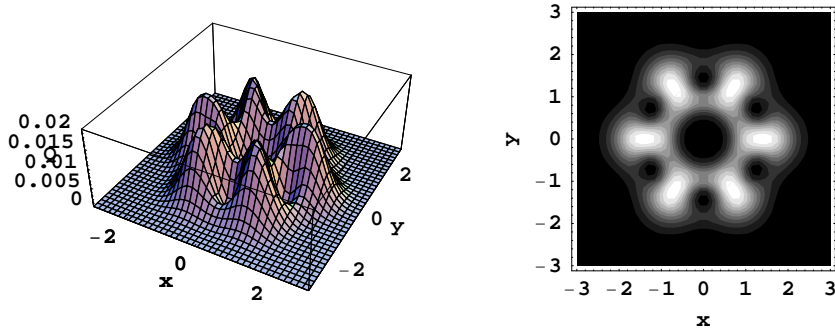


FIG. 9: Function  $Q = \pi^3 Q_{\xi pq}^{Kj}(x, y)$  and its contour plot for  $\xi = 5, p = q = 0, K = 2$  and  $j = 1$ .

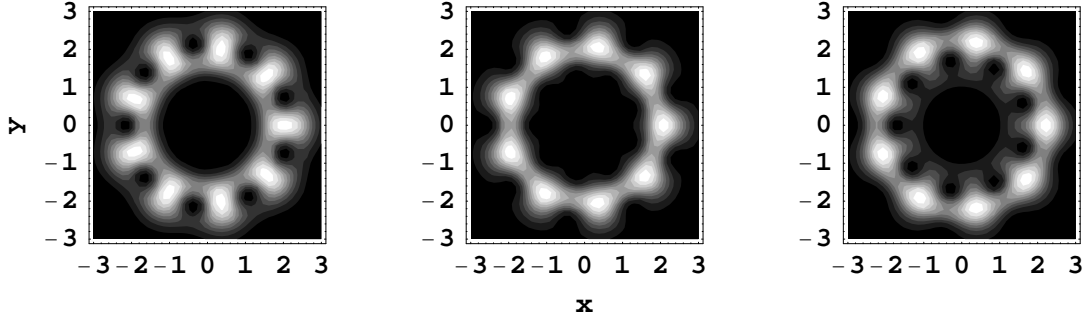


FIG. 10: Contour plots of  $Q = \pi^3 Q_{\xi pq}^{Kj}(x, y)$  for  $\xi = 12$ ,  $p = q = 0$ ,  $K = 3$  with  $j = 0$  ( left), 1 (middle) and 2 (right).

where  $\alpha, \beta, \gamma \in \mathcal{C}$  and  $|\alpha, \beta, \gamma\rangle_{abc} \equiv |\alpha\rangle_a |\beta\rangle_b |\gamma\rangle_c$  with  $|\alpha\rangle_a, |\beta\rangle_b, |\gamma\rangle_c$  the usual coherent states (18) of modes  $a, b, c$ . This function is non-negative definite, bounded and normalized to unity

$$\int \int \int Q_{\xi pq}^{Kj}(\alpha, \beta, \gamma) d^2 \alpha d^2 \beta d^2 \gamma = 1. \quad (51)$$

Generally there are six variables associated with the real and imaginary parts of  $\alpha, \beta$  and  $\gamma$ . For visualization let us confine ourselves to a subspace determined by  $\alpha = \beta = \gamma$ . In that subspace the Q-function for KTCS's is calculated to be

$$Q_{\xi pq}^{Kj}(x, y) = \frac{1}{\pi^3} N_{Kj}^2(\xi, p, q) e^{-3(x^2+y^2)} (x^2 + y^2)^{p+q} \left| N_{Kj}^{-2}(\xi(x - iy)^3, p, q) \right|^2 \quad (52)$$

with  $x = \text{Re}(\alpha)$  and  $y = \text{Im}(\alpha)$ . We represent in Figs. 8 and 9 the function  $Q_{\xi pq}^{Kj}(x, y)$  and its contour plot for  $K = 2$ ,  $j = 0$  and 1. The figures clearly manifest signatures of Schrödinger-cat-like states: constructive (Fig. 8) and destructive (Fig. 9) interference fringes between bell-like peaks (there are  $3K$  bells for a given  $K$ ). The  $K = 2$  state with  $j = 0$  ( $j = 1$ ) is called even (odd) trio coherent state [54, 55]. We also present in Fig. 10 contour plots of the case of  $K = 3$  with  $j = 0, 1$  and 2 which shows nine interfering bells. Transparently the pronounced interference fringe structures are  $j$ -dependent. It is the phase-space quantum interferences between different TCS's (instead of being simply added) that bring about copious nonclassical signatures of the KTCS.

#### 4. Physical realization

After having studied physical properties of KTCS's we proceed to find ways to realize them. In this section we are concerned with the context of ion trap. Since ions can be trapped very efficiently and their entanglement with the environment is extremely weak, trapped ions have advantages for many purposes such as preparing various types of nonclassical states (see e.g. [56, 57, 58, 59, 60, 61, 62]), simulating nonlinear interactions [63], demonstrating quantum phase transitions [64, 65], establishing quantum search algorithms [66] and so on. The most promising merit of trapped ion systems is perhaps the possibility to implement scalable quantum computers [67] in which a number of ions are involved [68, 69, 70]. Nevertheless, many tasks can still be done even with a single ion. For instance, a controlled-NOT quantum logic gate can be performed just by a single trapped ion [71, 72, 73, 74]: the target qubit is stored in the ion internal electronic states while the external quantized motional states, i.e. the phonon states, of the same ion serves as the control qubit. Here we propose an experimental scheme to generate KTCS's with  $K = 2$  in the vibronic motion of an ion which is trapped in real three-dimensional ( $3D$ ) space. The situations corresponding to  $1D$  and  $2D$  were already considered in [75] and [76] for the single- and two-mode case, respectively.

We first trap a two-level ion of mass  $M$  by a  $3D$  isotropic harmonic potential characterized by the trap (phonon) frequency  $\nu$ . Let  $\hat{a}, \hat{b}$  and  $\hat{c}$  be the phonon annihilation operator in the  $x$ -,  $y$ - and  $z$ -axis, respectively. The ion is then simultaneously driven by fourteen traveling-wave lasers (compare with the TCS case [35]) in the resolved sideband regime. The first thirteen lasers are all tuned to be resonant with the sixth red motional sideband, i.e. their frequency is  $\omega = \Delta - 6\nu$  with  $\Delta$  the energy difference between the two electronic levels of the ion. For our purpose it is essential that the lasers be judiciously configured. Namely, we shine the 1st (2nd, 3rd, 4th, 5th, 6th, 7th, 8th, 9th, 10th, 11th, 12th and 13th ) laser along the direction connecting the coordinate origin  $\{x, y, z\} = \{0, 0, 0\}$  to a point

$\{x, y, z\} = \{1, 1, 1\}$  ( $\{1, -1, 1\}, \{1, 1, -1\}, \{1, -1, -1\}, \{1, 1, 0\}, \{1, -1, 0\}, \{1, 0, 1\}, \{1, 0, -1\}, \{0, 1, 1\}, \{0, 1, -1\}, \{1, 0, 0\}, \{0, 1, 0\}$  and  $\{0, 0, 1\}$ ). As for the 14th laser, it must be in resonance with the electronic transition, i.e. its frequency is equal to  $\Delta$ , but its propagation direction is unimportant. The Hamiltonian of the ion-phonon-laser system is ( $\hbar = 1$ )

$$H = \frac{\Delta}{2}\sigma_z + \nu(\widehat{a}^\dagger\widehat{a} + \widehat{b}^\dagger\widehat{b} + \widehat{c}^\dagger\widehat{c}) + H_{int} \quad (53)$$

where

$$H_{int} = \sum_{l=1}^{14} \left[ \Omega_l \exp[-i(\omega_l t + \varphi_l) + i\mathbf{k}_l \widehat{\mathbf{R}}_l] \sigma_+ + \text{H.c.} \right] \quad (54)$$

with  $\Omega_l$  the Rabi frequencies,  $\omega_{1,2,\dots,13} = \omega$ ,  $\omega_{14} = \Delta$ ,  $\varphi_l$  the phases,  $\widehat{\mathbf{R}}_l$  the position operator along the laser direction determined by the wave vector  $\mathbf{k}_l$ ,  $\sigma_z = |e\rangle\langle e| - |g\rangle\langle g|$ ,  $\sigma_+ = \sigma_-^\dagger = |e\rangle\langle g|$  and  $|g\rangle$  ( $|e\rangle$ ) the ion's electronic ground (excited) state. Assuming  $k_l = k \forall l$  there is a single Lamb-Dicke parameter  $\eta = k/\sqrt{2M\nu}$  which measures the localization of the ion relative to the laser wavelength. In terms of  $\eta$  we obtain, in an interaction picture with respect to  $H_0 = H - H_{int}$ , the interaction Hamiltonian of the form

$$\mathcal{H}_{int} = e^{-\eta^2/2} \sum_{m=0}^{\infty} \frac{(-\eta^2)^m}{m!} \left[ -\eta^6 \sum_{l=1}^{13} \Omega_l e^{-i\varphi_l} \frac{(\widehat{A}_l^\dagger)^m \widehat{A}_l^{m+6}}{(m+6)!} + \Omega_{14} e^{-i\varphi_{14}} \frac{(\widehat{A}_{14}^\dagger)^m \widehat{A}_{14}^m}{m!} \right] \sigma_+ + \text{H.c.} \quad (55)$$

In the Lamb-Dicke limit  $\eta \ll 1$  we can retain only the  $m = 0$  term in (55) and reduce it to

$$\mathcal{H}_{int} = \left[ -\frac{\eta^6}{6!} \sum_{l=1}^{13} \Omega_l e^{-i\varphi_l} \widehat{A}_l^6 + \Omega_{14} e^{-i\varphi_{14}} \right] \sigma_+ + \text{H.c.} \quad (56)$$

Thanks to our configuration for the lasers the operators  $\widehat{A}_{1,2,\dots,13}$  are expressed through  $\widehat{a}$ ,  $\widehat{b}$  and  $\widehat{c}$  as

$$\widehat{A}_{1,2} = \widehat{a} \pm \widehat{b} + \widehat{c}, \quad \widehat{A}_{3,4} = \widehat{a} \pm \widehat{b} - \widehat{c}, \quad (57)$$

$$\widehat{A}_{5,6} = \widehat{a} \pm \widehat{b}, \quad \widehat{A}_{7,8} = \widehat{a} \pm \widehat{c}, \quad \widehat{A}_{9,10} = \widehat{b} \pm \widehat{c}, \quad (58)$$

$$\widehat{A}_{11} = \widehat{a}, \quad \widehat{A}_{12} = \widehat{b}, \quad \widehat{A}_{13} = \widehat{c}. \quad (59)$$

If we control the laser intensities and phases in such a way that

$$\Omega_{1,2,3,4} = \frac{1}{2}\Omega_{5,6,7,8,9,10} = \frac{1}{4}\Omega_{11,12,13} = \Omega, \quad (60)$$

$$\varphi_{1,2,3,4} = \varphi_{11,12,13} = \varphi + \pi, \quad \varphi_{5,6,7,8,9,10} = \varphi, \quad \varphi_{14} = \pi, \quad (61)$$

then use of Eqs. (57) - (59) in (56) yields

$$\mathcal{H}_{int} = \zeta \left[ (\widehat{abc})^2 - \xi^2 \right] \sigma_+ + \text{H.c.}, \quad (62)$$

thanks to the identity

$$\sum_{l=1}^4 \widehat{A}_l^6 - 2 \sum_{m=5}^{10} \widehat{A}_m^6 + 4 \sum_{n=11}^{13} \widehat{A}_n^6 \equiv 360(\widehat{abc})^2. \quad (63)$$

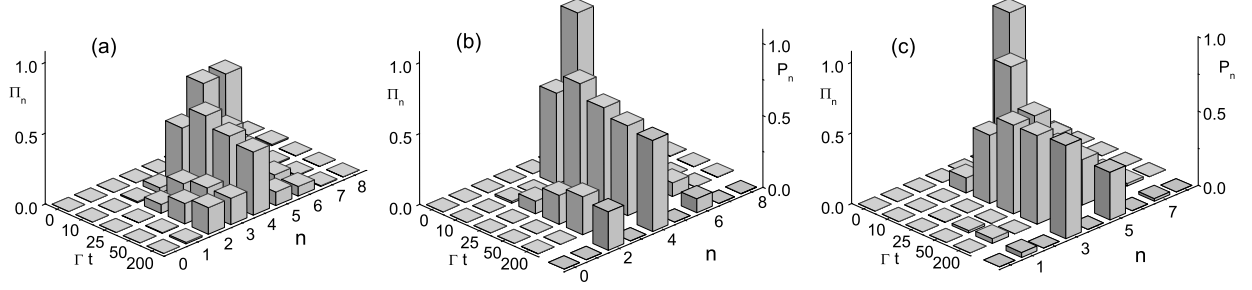


FIG. 11: 3D bar plots of phonon number distribution  $\Pi_n$  at different values of  $\Gamma t$  for  $\xi = 8$ ,  $p = q = 0$ ,  $\zeta = 0.02$  and  $l = 3$ . (a)  $w = 0.5$ : no KTCS's are generated since in the long-time limit  $\Pi_n$  is non-zero at both even and odd  $n$ , i.e. it does not display required oscillation. (b)  $w = 0$ : generation of state  $|\xi, p, q\rangle_{20}$  is justified in the long-time limit by coincidence of  $\Pi_n$ , Eq. (72), with  $P_n \equiv P_n(\xi, p, q, 2, 0)$ , Eq. (34). (c)  $w = 1$ : generation of state  $|\xi, p, q\rangle_{21}$  is justified in the long-time limit by coincidence of  $\Pi_n$ , Eq. (72), with  $P_n \equiv P_n(\xi, p, q, 2, 1)$ , Eq. (34).

The Hamiltonian (62) is the central result for the physical realization under consideration. The new parameters  $\zeta$ ,  $\xi$  appearing in (62) are controllable and given simply by

$$\zeta = \frac{\Omega\eta^6}{2} \exp(-i\varphi), \quad (64)$$

$$\xi^2 = \frac{2\Omega_{14}}{\Omega\eta^6} \exp(i\varphi). \quad (65)$$

Since the trapped ion is well isolated the dominant channel of decoherence is via the spontaneous decay. Then the time evolution of the system density operator  $\rho$  is governed by the following master equation

$$\frac{d\rho}{dt} = -i[\mathcal{H}_{int}, \rho] + \Gamma \left( \sigma_- \rho \sigma_+ - \frac{\sigma_+ \sigma_- \rho}{2} - \frac{\rho \sigma_+ \sigma_-}{2} \right) \quad (66)$$

where  $\Gamma$  accounts for the spontaneous decay rate of the ion being in its electronic excited state  $|e\rangle$ .

It is clear that the system ceases to evolve when the ion's fluorescence stops. Hence, the "dark" stationary solution of Eq. (66) in the long-time limit has the ansatz

$$\rho(\infty) = |g\rangle |\Psi\rangle_{xyz} \langle\Psi| \langle g| \quad (67)$$

where  $|\Psi\rangle_{xyz}$  solely determines the phonon state. Setting  $d\rho(\infty)/dt = 0$  in Eq. (66) and using properties of the operators  $\sigma_{\pm}$  we arrive at an equation for  $|\Psi\rangle_{xyz}$ ,

$$(\widehat{a}\widehat{b}\widehat{c})^2 |\Psi\rangle_{xyz} = \xi^2 |\Psi\rangle_{xyz}, \quad (68)$$

where  $\xi^2$  depends on the experiment parameters via (65).

For  $|\Psi\rangle_{xyz}$  to be a desired KTCS  $|\xi, p, q\rangle_{20}$  or  $|\xi, p, q\rangle_{21}$  we need to prepare an appropriate initial state. Furthermore, the generation time is influenced by all the parameters involved. To see these let us simulate Eq. (66) by the Monte Carlo Wave-Function approach [77] with an initial state of the form

$$|\Phi_w(0)\rangle = |e\rangle \left( \sqrt{w} |\Psi_{10}\rangle_{xyz} + \sqrt{1-w} |\Psi_{11}\rangle_{xyz} \right) \quad (69)$$

where  $0 \leq w \leq 1$  and

$$|\Psi_{1j}\rangle_{xyz} = |2l + q + j\rangle_x |2l + p + j\rangle_y |2l + j\rangle_z \quad (70)$$

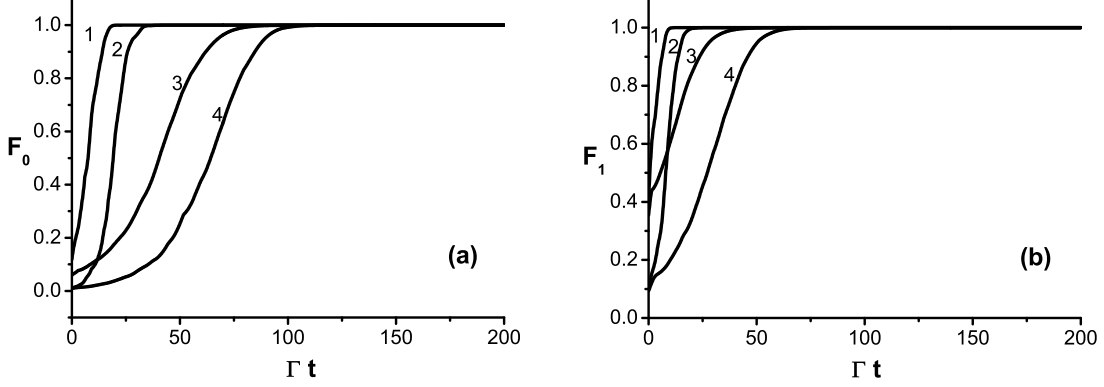


FIG. 12: Fidelities (a)  $F_0$  and (b)  $F_1$  as a function of  $\Gamma t$  for different sets of parameters: Curves 1, 2, 3 and 4 correspond to  $\{\xi, \zeta/\Gamma, p = q, l\} = \{10, 0.005, 2, 0\}$ ,  $\{10, 0.005, 0, 0\}$ ,  $\{6, 0.005, 0, 0\}$  and  $\{10, 0.002, 0, 0\}$ , respectively.

with a non-negative integer  $l$  and  $j = 0$  or  $1$ . Since the dynamics under consideration does not mix the parity, at time  $t > 0$  we have

$$|\Phi_w(t)\rangle = \sum_{m=0}^{\infty} (G_m(t) |g\rangle + E_m(t) |e\rangle) \left( \sqrt{w} |\Psi_{m0}\rangle_{xyz} + \sqrt{1-w} |\Psi_{m1}\rangle_{xyz} \right) \quad (71)$$

where  $G_m$  and  $E_m$  are some time-dependent coefficients to be simulated. In Fig. 11 we plot the phonon number distribution

$$\Pi_n(t) = \left| \langle \Phi_w(t) | n+q \rangle_x | n+p \rangle_y | n \rangle_z \right|^2 \quad (72)$$

at different times. Obviously, for  $0 < w < 1$ ,  $\Pi_n$  may be nonzero at any  $n$ . In particular, for  $w = 0.5$  there is no oscillation at all in  $\Pi_n$  in the long-time limit (see Fig. 11 (a)). Thus, a desired KTCS  $|\xi, p, q\rangle_{20}$  or  $|\xi, p, q\rangle_{21}$  results only when either  $w = 0$  or  $w = 1$  as seen from Fig. 11 (b) or Fig. 11 (c). These figures show that in the course of time the phonon number distribution  $\Pi_n(t)$  changes gradually and finally tends to coincide with  $P_n(\xi, p, q, 2, 0)$  if  $w = 0$  (Fig. 11 (b)) or with  $P_n(\xi, p, q, 2, 1)$  if  $w = 1$  (Fig. 11 (c)), implying successful generation of the target state  $|\xi, p, q\rangle_{20}$  or  $|\xi, p, q\rangle_{21}$ .

To assess quality of the resulting state as well as the generation time of our scheme we examine time-dependence of the fidelity

$$F_j(t) = |\langle \Phi_j(t) | \xi, p, q \rangle_{2j}|^2. \quad (73)$$

In Fig. 12 we represent  $F_j$  as a function of  $\Gamma t$  for various sets of parameters. Although initially the transient behaviors happen differently for different parameters' sets, after some period of time a stationary regime is inevitably established in all cases. It also follows from the figure that the generation time, i.e. the time needed to reach the stationary regime, is shorter for greater  $p, q$  (compare Curves 1 and 2),  $\xi$  (compare Curves 2 and 3) as well as  $\zeta$  (compare Curves 2 and 4). For a wide range of parameters we find out that  $1 - F_j$  becomes less than  $10^{-3}$  for  $\Gamma t \geq 200$ . The desired KTCS is thus produced with high purity within a relatively short period of time (compared, e.g., with the TCS generation time [35]). The KTCS obtained in our scheme is also stable since its appearance is accompanied by the “dark” ion which is to be found in the ground state  $|g\rangle$  and therefore does not interact with the laser fields any longer.

## 5. Conclusion

We have introduced and studied KTCS's which are both higher-order and multimode. Being superposed of phase-correlated TCS's, a KTCS is indeed a new physical state as dictated by the quantum mechanics superposition principle. The novel nonclassical features of KTCS's, as compared to TCS's, were demonstrated in detail and an

experimental generation scheme for  $K = 2$  was also presented in the ion trap context. Since these KTCS's are entangled states, they do promise potential implementations in quantum information processing and quantum computation. In particular, their three-mode nature would be crucial for tasks such as quantum controlled teleportation or/and quantum telecloning of certain types of continuous-variable states as well as inequality-free "one-shot" tests of local hidden-variable theories, etc. Such applications of KTCS's are being under way and will be reported elsewhere.

### Acknowledgments

The authors thank the KIAS Quantum Information Group for useful discussions. H.S.Y. was supported by R&D Program for Fusion Strategy of Advanced Technologies MI-0326-0830002, B.A.N. by KIAS R&D Fund No. 03-0149-002 and J.K. by Korea Research Foundation Grant No. KRF-2002-070-C00029.

- 
- [1] van Loock P and Braunstein S L 2000 *Phys. Rev. Lett.* **84** 3482
  - [2] Nguyen B A 2003 *Phys. Rev. A* **68** 022321
  - [3] van Loock P and Braunstein S L 2001 *Phys. Rev. Lett.* **87** 247901
  - [4] Lynch R 1994 *Phys. Rev. A* **49** 2800
  - [5] Nguyen B A 2001 *Phys. Lett. A* **284** 72
  - [6] Truong M D and Nguyen B A 2004 *J. Korean Phys. Soc.* **44** 1421
  - [7] Nguyen B A and Truong M D 2002 *J. Phys. A: Math. Gen.* **35** 4749
  - [8] Buzek V, Jex I and Quang T 1990 *J. Mod. Opt.* **37** 159
  - [9] Sun J, Wang J and Wang C 1992 *Phys. Rev. A* **46** 1700
  - [10] Jose W D and Mizrahi S S 2000 *J. Opt. B: Quantum Semiclass. Opt.* **2** 306
  - [11] Liu X M 1999 *J. Phys. A: Math. Gen.* **32** 8685
  - [12] Nieto M M and Truax D R 2000 *Opt. Commun.* **179** 197
  - [13] Manko V I, Marmo G, Porzio A, Solimeno S and Zaccaria F 2000 *Phys. Rev. A* **62** 053407
  - [14] Nguyen B A 2001 *Chin. J. Phys.* **39** 594
  - [15] Gerry C C and Grobe R 1995 *Phys. Rev. A* **51** 1698
  - [16] Gou S C, Steinbach J and Knight P L 1996 *Phys. Rev. A* **54** 4315
  - [17] Liu X M 2001 *Phys. Lett. A* **279** 123
  - [18] Liu X M 2001 *Phys. Lett. A* **292** 23
  - [19] Dodonov V V 2002 *J. Opt. B: Quantum Semiclass. Opt.* **4** R1
  - [20] Hillery M 1989 *Phys. Rev. A* **40** 3147
  - [21] Nguyen B A and Vo T 1999 *Phys. Lett. A* **261** 34
  - [22] Nguyen B A and Vo T 2000 *J. Phys. A: Math. Gen.* **33** 2951
  - [23] Nguyen B A and Vo T 2000 *Phys. Lett. A* **270** 27
  - [24] Agarwal G S 1986 *Phys. Rev. Lett.* **57** 827
  - [25] Tara K and Agarwal G S 1994 *Phys. Rev. A* **50** 2870
  - [26] Gilchrist A, Deuar P and Reid M D 1998 *Phys. Rev. Lett.* **80** 3169
  - [27] Gilchrist A, Deuar P and Reid M D 1998 *Phys. Rev. A* **60** 4259
  - [28] Obada A-S F, Abdel-Khalek S and El-Shahat T M 2004 *J. Korean Phys. Soc.* **44** 836
  - [29] Mancini S and Tombesi P 2003 *Quantum Info. Compu.* **3** 106
  - [30] Li S-B, Wu R-K, Wang Q-M and Xu J-B 2004 *Phys. Lett. A* **325** 206
  - [31] Bhaumik D, Bhaumik K and Dutta-Roy B 1976 *J. Phys. A: Math. Gen.* **9** 1507
  - [32] Eriksson K E and Skagerstam B S 1979 *J. Phys. A: Math. Gen.* **12** 2175
  - [33] van Enk S J 2003 *Phys. Rev. Lett.* **91** 017902
  - [34] Nguyen B A and Truong M D 2002 *J. Opt. B: Quantum Semiclass. Opt.* **4** 80
  - [35] Yi H S, Nguyen B A and Kim J 2003 *Phys. Lett. A* **315** 6
  - [36] Sixdeniers J M and Penson K A 2001 *J. Phys. A: Math. Gen.* **34** 2859
  - [37] Akhiezer N I 1965 *The Classical Moment Problem and Some Related Questions in Analysis* (London: Oliver and Boyd)
  - [38] Ditkin V A and Prudnikov A P 1965 *Integral Transforms and Operational Calculus* (Oxford: Pergamon Press)
  - [39] Sneddon I N 1974 *The Use of Integral transforms* (New York: McGrawHill)
  - [40] Fernandez D J, Hussin V and Nieto L M 1994 *J. Phys. A: Math. Gen.* **27** 3547
  - [41] Sixdeniers J M, Penson K A and Solomon A J 1999 *J. Phys. A: Math. Gen.* **32** 7543
  - [42] Penson K A and Solomon A J 1999 *J. Math. Phys.* **40** 2354
  - [43] Sixdeniers J M and Penson 2000 *J. Phys. A: Math. Gen.* **33** 2907
  - [44] Klauder J R, Penson K A and Sixdeniers J M 2001 *Phys. Rev. A* **64** 013817
  - [45] Appl T and Schiller D H 2004 *J. Phys. A: Math. Gen.* **37** 2731
  - [46] Bender C M and Orszag S A 1978 *Advanced Mathematical Methods for Scientific and Engineers* (Singapore: McGraw and Hill)
  - [47] Prudnikov A P, Brychkov Yu A and Marichev O I 1990 More special functions *Integrals and Series* vol 3 (New York:



Gordon and Breach)

- [48] Klauder J R 1963 *J. Math. Phys.* **4** 1058
- [49] Klauder J R and Skagerstam B S 1985 *Coherent States, Applications in Physics and Mathematical Physics* (Singapore: World Scientific)
- [50] Mandel L and Wolf E 1995 *Optical Coherence and Quantum Optics* (Cambridge: Cambridge University Press)
- [51] London R 1980 *Rep. Prog. Phys.* **43** 58
- [52] Christopher C G and Rainer G 1995 *Phys. Rev. A* **51** 1698
- [53] Santos E 2003 *Eur. Phys. J. D* **22** 423
- [54] Nguyen B A and Truong M D 2002 *J. Opt. B: Quantum Semiclass. Opt.* **4** 289
- [55] Nguyen B A 2003 *Phys. Lett. A* **312** 268
- [56] Meekhof D M, Monroe C, King B E, Itano W M and Wineland D J 1996 *Phys. Rev. Lett.* **76** 1796
- [57] Monroe C, Meekhof DM, King B E and Wineland DJ 1996 *Science* **272** 1131
- [58] Munro W J, Milburn G J and Sanders B C 2000 *Phys. Rev. A* **62** 052108
- [59] Kis Z, Vogel W and Davidovich L 2001 *Phys. Rev. A* **64** 033401
- [60] Solano E, de Matos Filho R L and Zagury N 2001 *Phys. Rev. Lett.* **87** 060402
- [61] Solano E, de Matos Filho R L and Zagury N 2002 *J. Opt. B: Quantum Semiclass. Opt.* **4** S324
- [62] Nguyen B A and Truong M D 2002 *Int. J. Mod. Phys. B* **16** 519
- [63] Milburn G J 1999 quant-ph/9908037
- [64] Porras D and Cirac J I 2004 quant-ph/0401102
- [65] Barjaktarevic J P, Milburn G J and McKenzie R H 2004 quant-ph/0401137
- [66] Agarwal G S, Ariunbold G O, Zanthier J V and Walther H 2004 quant-ph/0401141
- [67] Cirac J I and Zoller P 1995 *Phys. Rev. Lett.* **74** 4091
- [68] Schmidt-Kaler F, Haffner H, Riebe M, Gulde S, Lancaster G P T, Deuschle T, Becher C, Roos C F, Eschner J and Blatt R 2003 *Nature* **422** 408
- [69] Liebfried D, Demarco B, Meyer V, Lucas D, Barret M, Britton J, Itano W M, Jelenkovi B, Langer C, Rosenband T and Wineland D J 2003 *Nature* **422** 412
- [70] Beige A 2004 *Phys. Rev. A* **69** 012303
- [71] Monroe C, Meekhof D M, King B E, Hano W M and Wineland D J 1995 *Phys. Rev. Lett.* **75** 4714
- [72] Monroe C, Leibfried D, King B E, Meekhof D M, Itano W M and Wineland D J 1997 *Phys. Rev. A* **55** R2489
- [73] Childs A M and Chuang I L 2000 *Phys. Rev. A* **63** 012306
- [74] Wei L F and Lei X L 2000 *J. Opt. B: Quantum Semiclass. Opt.* **2** 581
- [75] de Matos Filho R L and Vogel W 1996 *Phys. Rev. Lett.* **76** 608
- [76] Gou S C, Steinbach J and Knight P L 1996 *Phys. Rev. A* **54** 4315
- [77] Dalibard J, Castin Y and Molmer K 1992 *Phys. Rev. Lett.* **68** 580